Available online at www.eccomasproceedia.org
Eccomas Proceedia UNCECOMP (2025) 278-292

ECCOMAS
Proceedia

UNCECOMP 2025
6th ECCOMAS Thematic Conference on
Uncertainty Quantification in Computational Science and Engineering
M. Papadrakakis, V. Papadopoulos, G. Stefanou (eds.)
Rhodes Island, Greece, 15-18 June 2025

UPDATING DIGITAL TWINS SUBJECTED TO UNCERTAIN CORROSION CONDITIONS USING THE UNSCENTED KALMAN FILTER METHOD

Ioannis A. Prentzas[1], **Spyridon G. Diamantopoulos**, [1], **Alexandros D. Michailidis**[1], **and Michalis Fragiadakis**[1]

[1] National Technical University of Athens, School of Civil Engineering
address
e-mail: {gprentzas, sdiamadop, alex_michailidis, mfrag}@mail.ntua.gr

Abstract. *The paper presents a framework for updating models of reinforced concrete (RC) structures due to aging effects. This is accomplished through a nonlinear finite element model (FEM) updating procedure using the Unscented Kalman Filter (UKF) method. The UKF method recursively updates the FEM by integrating new information, resulting in a more realistic representation of the structure over time. Specifically, corrosion-related parameters, such as material degradation and the loss of reinforcement cross-sectional area, are updated based on measurements. The measurements have been generated using probabilistic models to ensure that structural analysis accounts for the progressive deterioration caused by chloride-induced corrosion in RC bridges. The efficiency of various measurement types is examined. Additionally, parametric studies are conducted to investigate how varying corrosion levels and seismic intensities influence the updating procedure. The updated FEM model is subsequently adopted to generate fragility curves that explicitly incorporate the effects of structural aging on performance. The developed framework is applied to a bridge pier in order to evaluate the effectiveness of the proposed methodology for updating the reliability assessments models in the case of aging. A bridge case study is considered in order to demonstrate how the approach effectively considers corrosion effects and seismic performance, providing valuable decision-making regarding bridge maintenance, repair, and retrofit.*

Keywords: Reliability analysis, Unscented Kalman Filter, Aging, Model updating, recursive filte

doi: 10.7712/120225.12356.22057

1 INTRODUCTION

Reinforced concrete (RC) structures deteriorate progressively due to aging, environmental exposure, and prior loading events. Among the various degradation mechanisms, reinforcement corrosion is both the most widespread and one of the most detrimental, especially in marine and coastal regions where chloride ingress accelerates its initiation and propagation. The loss of steel cross-section, reduction in mechanical properties, and associated cracking of the surrounding concrete significantl alter the strength, stiffness, and energy dissipation capacity of RC members. In seismically active regions, these corrosion-induceddeficiencie accumulate over time, leaving structures more vulnerable to earthquakes and raising serious concerns about their long-term safety and serviceability.

This dual challenge of deterioration and seismic demand underscores the need for robust methods that can capture the evolving properties of corroded RC structures and provide reliable predictions of their seismic performance. Conventional assessment approaches often neglect deterioration or treat it deterministically, which limits their ability to quantify uncertainty and identify critical parameters. To overcome these limitations, finite-elemen model updating (FEMU) combined with probabilistic deterioration models provides a powerful framework for condition assessment. In particular, the Unscented Kalman Filter (UKF) [1] enables online nonlinear model updating, allowing for real-time estimation of corrosion-related parameters and improved fragility assessment of RC structures subjected to seismic loading.

Accurate estimation of corrosion-related parameters [3] through structural health monitoring or inspection is crucial for reliable seismic safety assessments and informed decision-making regarding repair, retrofit or demolition. Model updating [2] using fiel measurements (e.g., vibration data) offers a viable alternative, as it facilitates the creation of digital twins for performance prediction and maintenance planning [4]. Many previous studies have used model updating to estimate corrosion damage; however, most relied on linear finit element (FE) models and low-amplitude ambient or service loads, rendering them unsuitable for highly nonlinear seismic scenarios [5, 6]. These methods fail to account for complex hysteretic behavior and thus are inadequate for predicting performance under earthquakes.

To address this gap, this study presents a methodology that integrates nonlinear finit element model updating (FEMU) with seismic data, focusing on estimating corrosion-related parameters in RC structures. The proposed approach employs a stochastic inference technique, specificall the Unscented Kalman Filter (UKF), which updates the parameters in real time based on recorded seismic responses [7, 8, 9].

In this study, a nonlinear fibe -based finit element model is developed in the *OpenSeesPy* framework to simulate the seismic response of corroded RC bridge piers. Corrosion-induceddeterioration is incorporated by probabilistically reducing the steel reinforcement area and yield strength, while the concrete is modeled with nonlinear fibe sections to capture stiffness and strength degradation. Beyond reproducing the structural response, the framework integrates finite-elemen model updating with reliability analysis [10, 11], enabling the calibration of corrosion-related parameters and the subsequent updating of fragility curves. This combined approach allows not only accurate simulation of deterioration mechanisms but also improved assessment of the seismic reliability of aging RC piers. By means of simulated case studies incorporating different measurement noise type and ground motion intensities, this study shows that corrosion-related parameter changes—typically difficul to observe directly—can be successfully identified The goal is to establish a robust, model-based framework that enhances seismic performance assessment and supports risk-informed decision-making for the management of aging RC infrastructure.

2 DIGITAL UPDATING UPDATING FRAMEWORK FOR UNCERTAIN CORROSION CONDITIONS

The proposed framework uses Unscented Kalman Filter method to update crucial parameters of FEM model. Especially, corrosion-related parameters are of great interest. For this reason different corrosion induced scenario seismic measurements are produced using probabilistic corrosion models to vadilate the proposed framework. Utilizing recorded seismic data, the model's outputs are compared with observed responses through a Bayesian estimation process, such as the Unscented Kalman Filter (UKF). This model incorporates corrosion-affected parameters, which are initially unknown. The FE model, characterized by corrosion-related variables, is then iteratively updated to minimize discrepancies between simulated and observed responses, allowing for statistical inference of the unknown corrosion-induced properties. It is important to note that this approach necessitates advanced FE modeling techniques capable of capturing the complex effects of corrosion. Notably, it contributes to the refinemen of fragility curves, which quantify the probability of reaching or exceeding different damage levels during earthquakes. Prior to discussing the modeling of corroded RC members, a concise overview of the UKF method—central to estimating corrosion-related parameters—is presented.

2.1 Nonlinear FE Model Updating using Uscented Kalman Filter

An online nonlinear FE model can be used to estimate the response of a structure subjected to dynamic excitation by the nonlinear differential equation:

$$\mathbf{M}(\theta)\ddot{\mathbf{u}}_{k+1}(\theta) + \mathbf{C}(\theta)\dot{\mathbf{u}}_{k+1}(\theta) + \mathbf{r}(\mathbf{u}_{k+1}, \boldsymbol{\theta}) = \mathbf{p}_{k+1} \tag{1}$$

where $\mathbf{u}_{k+1}$, $\dot{\mathbf{u}}_{k+1}$, $\ddot{\mathbf{u}}_{k+1} \in \mathbb{R}^n$ (relative displacement, velocity, and acceleration response vectors, respectively), $\mathbf{M} \in \mathbb{R}^{n\times n}$ (mass matrix), $\mathbf{C} \in \mathbb{R}^{n\times n}$ (damping matrix), $\mathbf{r}(\mathbf{q}_{k+1},\ \boldsymbol{\theta})\mathbb{R}^n$ (resisting force vector), n = number of degrees of freedom (DOFs), $\boldsymbol{\theta} \in \mathbb{R}^{n\times 1}$ (vector of time-invariant model parameters), $\mathbf{p}_{k+1} = \mathbf{ML}\ddot{u}_{g,k+1}$, (dynamic load vector for rigid-base earthquake excitation), $\mathbf{L} \in \mathbb{R}^{n\times r}$ (influenc matrix), $\ddot{u}_{g,k+1} \in \mathbb{R}^{r\times 1}$ (input ground acceleration), r = number of base excitation components, k = 0, 1, . . . , N-1, where N is the number of data samples of the input ground acceleration record.

Then, different types of sensors can be deployed on the structure to measure different response quantities $\mathbf{y} \in \mathbb{R}^{n_y}$, where n_y denotes the number of measured responses. These responses can also be estimated from the nonlinear FE model. The measured and FE-predicted response quantities at time t_{k+1} can be related by [9]:

$$\mathbf{y}_{k+1} = \hat{y}_{k+1}(\boldsymbol{\theta}) + \mathbf{v}_{k+1} = \mathbf{h}_{k+1}(\boldsymbol{\theta}, \ddot{\mathbf{u}}^g_{1:k+1}) + \mathbf{v}_{k+1} \tag{2}$$

where $\mathbf{y}_{k+1} \in \mathbb{R}^{n_y}$ is the measured response at time t_{k+1}, $\hat{y}_{k+1}(\boldsymbol{\theta}) = \mathbf{h}_{k+1}(\boldsymbol{\theta}, \ddot{\mathbf{u}}^g_{1:k+1}) \in \mathbb{R}^{n_y}$ is the FE-predicted response with $\mathbf{h}_{k+1}(\cdot)$ referred to as the nonlinear response function, $\ddot{\mathbf{u}}^g_{1:k+1} = [(\ddot{\mathbf{u}}^g_1)^T, (\ddot{\mathbf{u}}^g_2)^T, \ldots (\ddot{\mathbf{u}}^g_{k+1})^T]^T$ is the input ground motion time history from time t_1 to t_{k+1} and $\mathbf{v}_{k+1} \in \mathbb{R}^{n_y}$ is the prediction error vector assumed here to be white Gaussian with zero-mean and diagonal covariance matrix $\mathbf{R}_{k+1}$, i.e., $\mathbf{v}_{k+1} \sim N(0, \mathbf{R}_{k+1})$. Note that 2 accounts for model parameter uncertainty and uncertainty related to input and response measurements; however, it does not explicitly account for model structure uncertainty, also referred to as modeling uncertainty. The model parameters to be estimated θ using UKF, can be modeled as a random walk, whose equation can be combined with Eq. 2 to defin the following non-linear state-space equation

$$\boldsymbol{\theta}_{k+1} = \boldsymbol{\theta}_k + \mathbf{w}_k \tag{3}$$

$$\mathbf{y}_{k+1} = \mathbf{h}_{k+1}(\boldsymbol{\theta}, \ddot{\mathbf{u}}^g_{1:k+1}) + \mathbf{v}_{k+1} \tag{4}$$

where $\mathbf{w}_k$ is the process noise assumed to be a white Gaussian with zero mean and diagonal covariance matrices $\mathbf{Q}_k$, i.e, $\mathbf{w} \sim N(\mathbf{0}, \mathbf{Q_k})$ and statistically uncorrelated with $\mathbf{v}_k$. In the proposed methodology, θ represents the unknown correlation-related properties and other model parameters, which are considered uncertain.

In this equation, $\mathbf{h}$ represents the simulated structure response until analysis step k, which is evaluated by analyzing the nonlinear FE model with the current estimate of model parameter vector θ_k, subjected to the seismic input characterized by earthquake ground motion acceleration series until the current time step k, i.e., $\ddot{u}_{g,1:k}$.

2.2 Probabilistic model of corroded RC piers

To predict the seismic response of corroded RC structures under extreme loading, a nonlinear finite-elemen (FE) model is required to evaluate $\mathbf{h}(\theta, \ddot{u}_g)$ in Eq. 2. Such a model must account for the influenc of corrosion on both geometric and material properties. In this study, corrosion is represented as a time-dependent, chloride-induced process, and a probabilistic framework is adopted to generate measurement data that reflec the variability and uncertainty associated with deterioration. The DuraCrete model [12] is adopted in this study to estimate the corrosion initiation time (T_{cor-in}). According to Stewart and Rosowsky [13], the early stage of reinforcement corrosion can be described using the one-dimensional form of Fick's second law. In this framework, the chloride concentration C is define as

$$\frac{\partial C(x,t)}{\partial t} = D\frac{\partial^2 C(x,t)}{\partial x^2}, \tag{5}$$

The solution to this equation is given by:

$$C(x,t) = C_s\left[1 - \text{erf}\left(\frac{x}{2\sqrt{Dt}}\right)\right]. \tag{6}$$

where $C(x,t)$ is the chloride concentration at depth x and exposure time t; D is the diffusion coefficient C_s is the surface chloride concentration; and erf$(\cdot)$ is the Gaussian error function. A widely adopted assumption is that reinforcement corrosion initiates once the chloride ion concentration at the depth of the concrete cover exceeds a critical threshold. Based on this concept, the corrosion initiation time ($T_{\text{cor-in}}$) can be estimated using the DuraCrete model [12]:

$$T_{\text{cor-in}} = X_l\left\{\frac{d_c^2}{4k_e k_t k_c D_0(t_0)^n}\left[\text{erf}^{-1}\left(1 - \frac{C_{\text{cr}}}{C_s}\right)\right]^{-2}\right\}^{\frac{1}{1-n}}. \tag{7}$$

where X_l is the modeling uncertainty factor; d_c is the reinforcement cover depth; k_e, k_c, and k_t are correction factors accounting for environmental conditions, curing time, and test methods,

Parameter	Distribution	Mean	St. dev.
d_c	Normal	38.1	11.4
k_e	Gamma	0.924	0.155
k_c	Beta	2.4	0.7
k_t	Normal	0.832	0.024
D_0	Normal	473	43.2 (10^{-12} mm^2/yr)
n	Beta	0.362	0.245
C_{cr}	Normal	0.90	0.15
C_{s} = Chloride surface concentration	—	(linear function of A_{cs} and ε_{cs} by weight of binder)	
A_{cs} = Parameter used in C_{s}	Normal	7.758	1.36
ε_{cs} = Parameter used in C_{s}	Normal	0	1.105

Table 1: Variables in the diffusion model used to estimate the corrosion initiation.

respectively; D_0 and t_0 are the reference diffusion coefficien and reference time; C_{cr} and C_s are the critical and surface chloride concentrations; and n is the aging factor.

Once corrosion initiates, the cross-sectional area of the reinforcing steel gradually decreases. Because this deterioration is time-dependent, it must be modeled as a function of exposure duration. Accordingly, a time-dependent expression is adopted to represent the evolution of the remaining diameter of the steel bar:

$$D_i(t) = \begin{cases} D_i, & t < T_{\text{cor-in}} \\ D_i - \alpha(t - T_{\text{cor-in}})^{0.71}, & T_{\text{cor-in}} \leq t \leq T_f \\ 0, & t > T_f, \end{cases} \tag{8}$$

where α is the deterioration factor, given by:

$$\alpha = \frac{1.0508 \times (1 - w/c) - 1.64}{d_c} \tag{9}$$

and w/c is the water-to-cement ratio.

$$T_f = T_{\text{cor-in}} + \frac{d_c \times D_i^{1/0.71}}{1.0508 \times (1 - w/c)^{-1.64}} \tag{10}$$

where D_i is the initial diameter of the ith reinforcing bar, T_f is the theoretical time at which D_i reduces to zero, and $D_i(t)$ is the time-dependent diameter. The corresponding mechanical properties of the corroded steel, accounting for the deterioration process, are expressed as:

$$f_y(t) = (1.0 - \alpha_y Q_{\text{corr}})\, f_{y0} \tag{11}$$

where f_{y0}, f_{u0}, and ϵ_{u0} are the yield strength, ultimate tensile strength, and ultimate elongation of the initial uncorroded steel bar, respectively. The term Q_{corr}, representing the averaged percentage of section loss, is given by

$$Q_{\text{corr}} = 100 \times \left\{ 1 - \left[\frac{D_i - D_i(t)}{D_i} \right]^2 \right\}. \tag{11}$$

3 FRAGILITY ASSESSMENT

Fragility curves are useful tools for assessing the seismic capacity of RC structures. The fragility of a system is the probability that an Engineering Demand Parameter, EDP, exceeds a threshold value, edp, and it is define as follows:

$$F_R(IM) = P(EDP > edp|IM) \tag{12}$$

Engineering demand parameters, $EDPs$, are quantities that characterize the system response, while IM is the Intensity Measure of interest. The EDPs usually considered for RC piers performance assessment are member plastic hinge rotation, or the Interstorey Drift Ratio (IDR), both parameters are directly related to the limit-state demand. Suitable IMs for piers are the Peak Ground Acceleration PGA, or preferably the spectral acceleration at the fundamental period $S_a(T_1, 5\%)$. For the present study, the EDP and the IM adopted are the maximum interstorey drift IDR and the firs mode spectral acceleration $S_a(T_1, 5\%)$.

If EDP values are known for given IM levels, assuming that the data follow a lognormal distribution, the probability of exceeding a limit-state threshold edp is given by the expression:

$$P(EDP \leq edp|IM) = \Phi\left[\frac{ln(EDP) - \mu_{lnEDP}}{\sigma_{lnEDP}}\right] \tag{13}$$

where Φ is the standard cumulative distribution function, σ_{lnEDP} is the logarithmic standard deviation of the logarithms of the EDP, and μ_{lnEDP} is the mean value of the logarithms of the EDP.

There are various approaches for calculating the fragility curves of Eq. 1. Figure 1 illustrates the different forms of engineering demand parameter–intensity measure (EDP–IM) data that can be used for fragility analysis, depending on the adopted methodology. Figure 1a presents a capacity curve, such as a force–displacement relationship obtained from seismic pushover analysis. In this format, the data directly describe the structural capacity as a function of demand, and fragility curves are derived by comparing capacity with seismic demand models. Figure 1b shows "stripped" data, where EDP values are provided conditionally at specifie IM levels, or conversely, IM values are recorded for fi ed EDP thresholds. This representation typically arises in incremental dynamic analysis (IDA) or stripe-based analysis, where ground motions are scaled to different intensity levels. The resulting horizontal or vertical bands of data facilitate direct estimation of fragility functions by quantifying the probability of exceeding predefine limit states at each IM level. Figure 1c illustrates the case where EDP–IM data form a random cloud, as is common in cloud analysis. Here, multiple nonlinear time-history analyses are performed using unscaled ground motions, producing scattered data points across the EDP–IM space. Statistical models, such as generalized linear regression or maximum likelihood estimation, are then employed to relate IM to the probability of exceeding a given EDP threshold. Together, these three formats—capacity, stripe, and cloud—represent the primary pathways to fragility calculation. The choice among them depends on the available data and the level of computational effort. In the present study, the cloud-type dataset is most relevant, as the simulated seismic responses of the corroded pier under varying input motions naturally generate scattered EDP–IM pairs, which can then be used to construct probabilistic fragility curves.

The approach followed in our study is based on the work of Fragiadakis and Vamvatsikos [14] who proposed an approximate method for estimating the median Incremental Dynamic Analysis (IDA) capacity curve and its fractiles from the backbone of the static pushover. Once the fractile IDAs are known, it is straightforward to calculate the fragility.

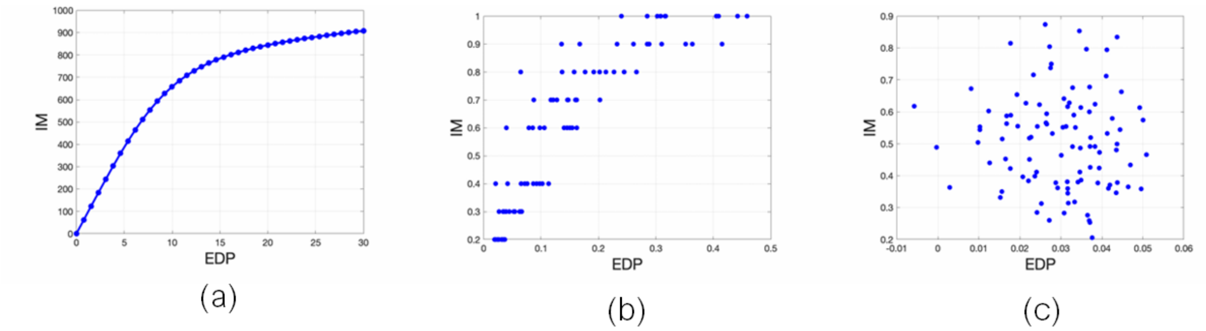

Figure 1: Different methods for creating fragility curves.

4 APPLICATION EXAMPLE

To test the proposed corrosion-related parameter estimation method, we apply it to a representative reinforced concrete (RC) bridge pier. Since fiel data on corroded RC piers under earthquakes are limited, we use numerical simulations instead. The pier is modeled in OpenSeesPy [15] and subjected to ground motions, and the resulting response histories—including the effects of corrosion—are treated as "measured" data for finite- lement model updating. We consider one corrosion scenario, define by different the initiation time and the exposure duration, under two seismic intensity levels, and perform a global sensitivity analysis to examine how well the key parameters can be identified

4.1 Example RC bridge pier model

The RC pier examined in this study is representative of highway bridges constructed prior to the adoption of modern seismic detailing standards. It has a hollow rectangular cross-section 2 above a fi ed foundation. The concrete, modeled using nonlinear fibe sections with the `Concrete01` material in OpenSeesPy, has a compressive strength of $f_c' = 25$ MPa, a Young's modulus of $E_c = 25$ GPa, and a Poisson's ratio of 0.2. The longitudinal reinforcement has a yield strength of $f_y = 415$ MPa. Rayleigh damping is applied to achieve 5% viscous damping. The pier is modelled using a force-based fibe -beam element to capture fl xural and shear responses under cyclic loading. Figure 2 shows the cross-section, with longitudinal bars and transverse ties, as well as the elevation view with element discretization, clarifying how the material and geometric properties are represented in the finite-elemen model.

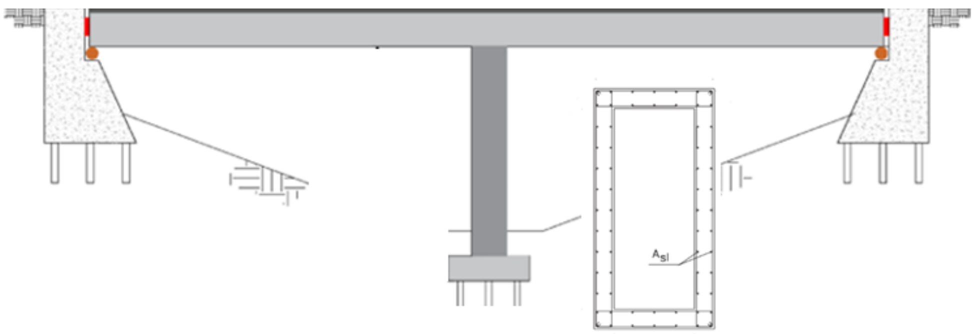

Figure 2: RC pier geometry: (a) cross-section showing longitudinal bars and transverse ties, (b) elevation view with element discretization.

4.2 Corrosion scenario - Seismic input

Corrosion effects are modeled using the probabilistic framework described in Section 2.2, where chloride ingress governs depassivation at $T_{\text{corr-in}}$ and subsequent deterioration develops during the aging period t_{aging}. The considered scenario represents a typical deterioration range, with corrosion initiated after 10 years and progressing over a 50-year aging period. The steel cross-sectional area and yield strength are reduced based on lognormal distributions that capture uncertainty in corrosion rates and spatial variability. These degraded properties are directly assigned to the reinforcement material definition in the FE model, allowing realistic simulation of stiffness and strength degradation.

To emulate fiel measurements, the corroded pier models are subjected to two scaled ground motions representative of low-to-moderate and high seismicity regions, corresponding to peak ground accelerations (PGAs) of $0.05g$ and $0.24g$, respectively. Each record is applied at the base in the longitudinal direction with a uniform time step of 0.005 s. Gaussian noise with a 2% standard deviation is superimposed on the signals to mimic sensor error and measurement variability. Figure 3a shows the acceleration time history for the mild corrosion scenario under the $0.05g$ and the $0.24g$ input.

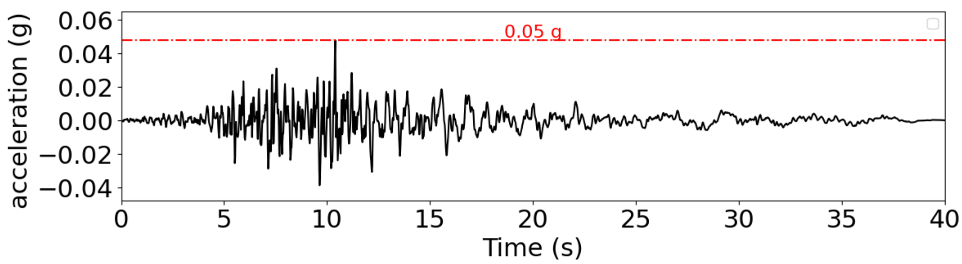

(a) Acceleration time history (pier top) for PGA = $0.05g$ under mild corrosion.

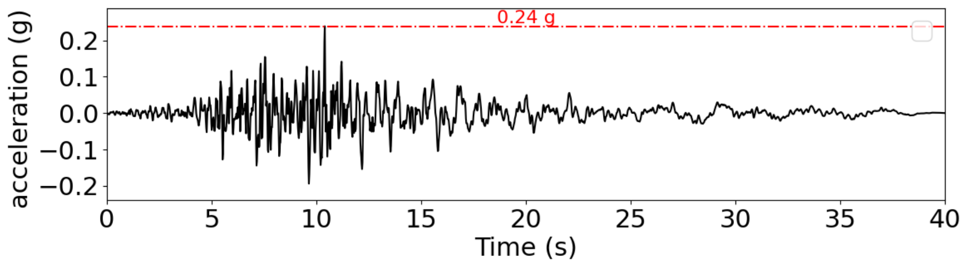

(b) Acceleration time history at pier top for PGA = $0.24g$ and mild corrosion.

Figure 3: Comparison of synthetic acceleration responses at the pier top under two seismic intensities: (a) PGA = $0.05g$, (b) PGA = $0.24g$.

4.3 Identifiability-sensitivity analysis

To determine which uncertain parameters most strongly influenc the seismic response metrics—or can be inferred from specifi measurements—we employ tornado diagrams. These diagrams are constructed by systematically perturbing each parameter by ±10% around its nominal value and quantifying the resulting change in peak acceleration. The parameters are then ranked according to their relative influence

Figures 4a and 4b present the sensitivity results for the 0.05g and 0.24g input levels, respectively. In both cases, the diameter of the steel reinforcement and the yield strength f_y are the dominant contributors to response variability, confirmin their importance as key corrosion-related parameters. At the lower 0.05g excitation, the pier response remains largely linear, which limits parameter identifiabilit to the rebar diameter. In contrast, under the higher 0.24g input, nonlinear effects are activated, allowing both the rebar diameter and yield strength to be identifie with confidence Subsequent figure further isolate the impact of these two parameters, showing the response variation under a ±10% perturbation at each intensity level.

From the perspective of finite-elemen model updating (FEMU), tornado diagrams provide a practical tool for prioritizing parameters: they highlight which properties are most likely to be identifiabl from the available measurements and therefore should be targeted in the updating process.

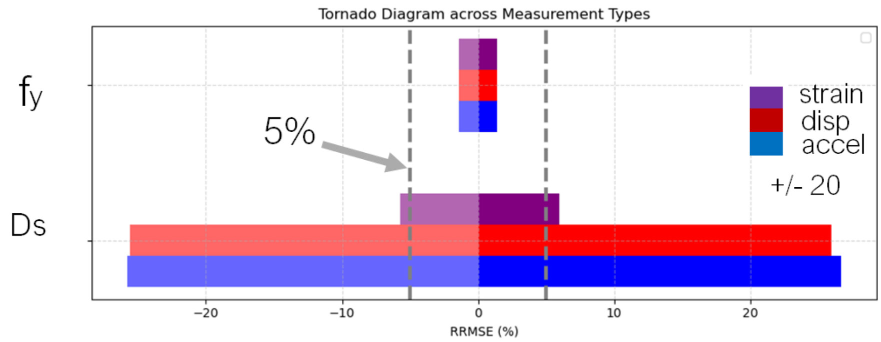

(a) Tornado sensitivity diagram for peak acceleration under PGA = 0.05g.

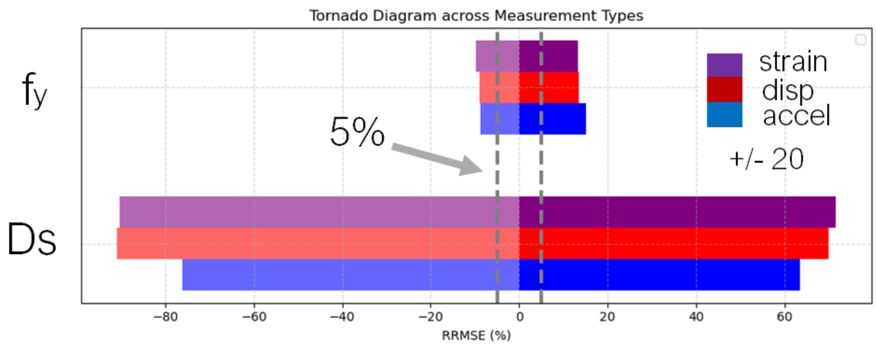

(b) Tornado sensitivity diagram for peak acceleration under PGA = 0.24g.

Figure 4: Comparison of tornado sensitivity diagrams for two seismic intensities: (a) PGA = 0.05g, (b) PGA = 0.24g.

4.4 Results for two ground motion intensity levels

Under the low-intensity 0.05g input, the mildly corroded pier primarily exhibits linear behavior, and as a result, the nonlinear parameters of the model cannot be reliably identified as illustrated by the tornado diagram in Figure 5. The sensitivity analysis indicates that only the diameter of the longitudinal steel reinforcement shows a measurable influenc on the seismic response at this intensity level. In particular, the estimation of the yield strength f_y requires a higher seismic intensity, since the pier must undergo nonlinear deformations before the effects of strength deterioration can be captured.

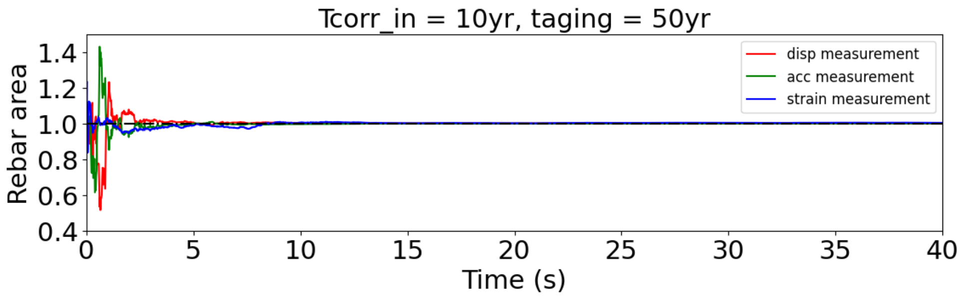

(a)

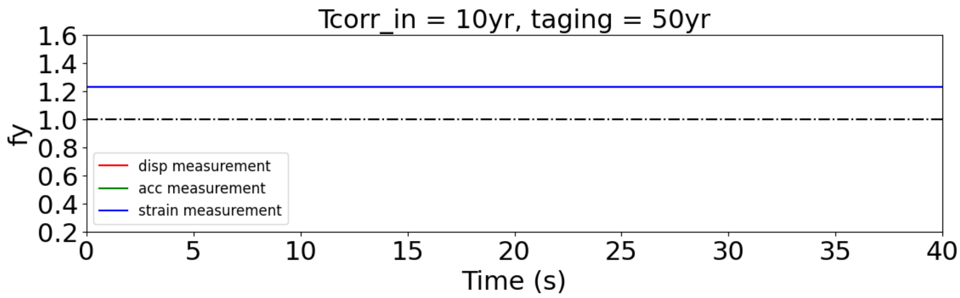

(b)

Figure 5: Convergence time-histories of the estimated unknown parameters (PGA = $0.05g$)

Under the higher-intensity $0.24g$ input, the mildly corroded pier develops a distinctly non-linear response, enabling the identificatio of parameters that cannot be captured under weaker excitation. Unlike the $0.05g$ case, where the response remained essentially linear and only the steel rebar diameter could be identified the stronger shaking activates inelastic mechanisms and makes it possible to identify both the diameter of the steel rebar and its yield strength. The sensitivity analysis confirm that these two reinforcement-related parameters dominate the variability in the seismic response, demonstrating their critical role in capturing the effects of corrosion-induced deterioration. Figure 4b illustrates their relative influenc under the $0.24g$ input, while Figures 6a and 6b show the congergence time-history for the rebar diameter and the yield strength, respectively.

These results highlight the importance of seismic intensity for parameter identifiabilit . At low levels, FEMU is restricted to identifying parameters linked to elastic stiffness, but at higher intensities, it can also capture nonlinear properties such as reinforcement strength. This underscores the need for strong-motion data in structural health monitoring applications, since only under sufficien excitation can the key corrosion-related parameters be reliably extracted and calibrated.

4.5 Unforeseen data

Figure 7 compares the drift ratio time histories predicted by the initial and updated FE models for the $0.05g$ input. As shown in Figure 7a, the initial model exhibits noticeable discrepancies relative to the reference corroded response, particularly in terms of peak amplitudes and phase

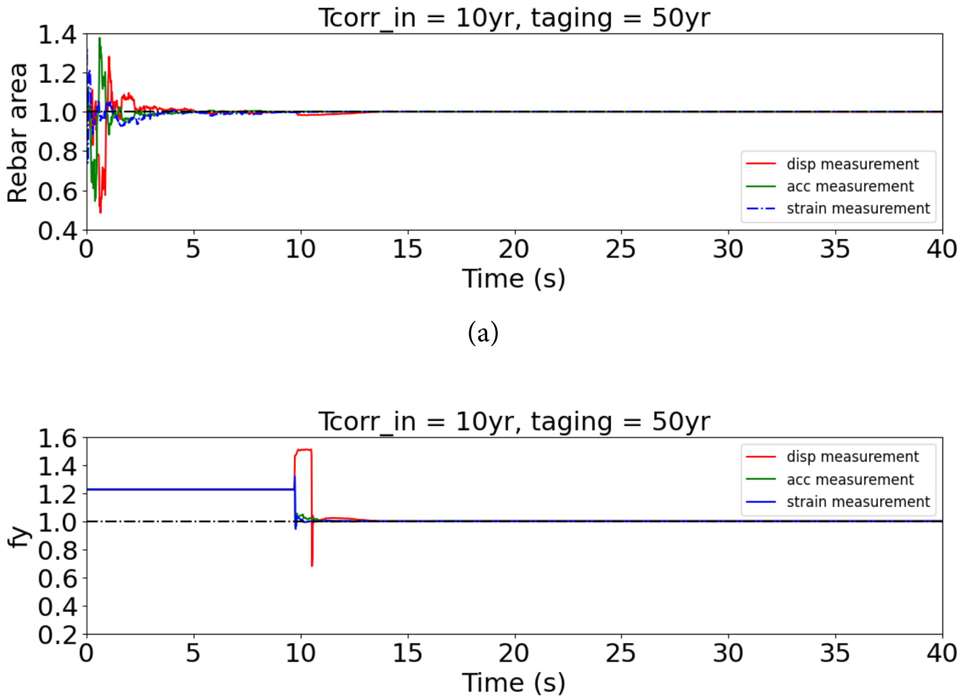

(a)

(b)

Figure 6: Convergence time-histories of the estimated unknown parameters (PGA = $0.24g$).

alignment, highlighting its limited predictive capability when corrosion-induced degradation is not properly accounted for. In contrast, Figure 7b demonstrates the substantial improvement achieved through model updating: the updated predictions across strain, acceleration, and displacement closely track the reference signals, capturing both the amplitude and timing of the structural response. Quantitatively, the root-mean-square (RMS) error decreases from 8.5% in the initial model to just 0.05% after updating, indicating a nearly exact reproduction of the measured response. This dramatic reduction in error confirm the effectiveness of the FEMU procedure in calibrating corrosion-affected parameters and restoring predictive accuracy. Moreover, Figure 7 illustrates the generalization capability of the updated model when subjected to an unseen ground motion (PGA = $0.05g$), further validating its robustness beyond the calibration dataset.

Figure 8 compares the drift ratio time histories predicted by the initial and updated FE models for the $0.24g$ input. As shown in Figure 8a, the initial model exhibits a pronounced mismatch with the reference corroded response, especially around peak drift values, where both the amplitude and phase deviate significantl . This discrepancy highlights the inability of the uncalibrated model to capture the combined effects of material deterioration and nonlinear cyclic behavior under stronger shaking. In contrast, Figure 8b illustrates the improved performance of the updated model, where predictions of strain, acceleration, and displacement align closely with the reference data across the entire response history. The root-mean-square (RMS) error is reduced from 46% with the initial model to just 0.10% after updating, underscoring the effectiveness of the FEMU procedure in calibrating key corrosion-related parameters. This substantial reduction not only confirm the accuracy of the updated model but also demonstrates its robustness when applied to higher seismic intensities, where nonlinearities and degradation effects are more pronounced.

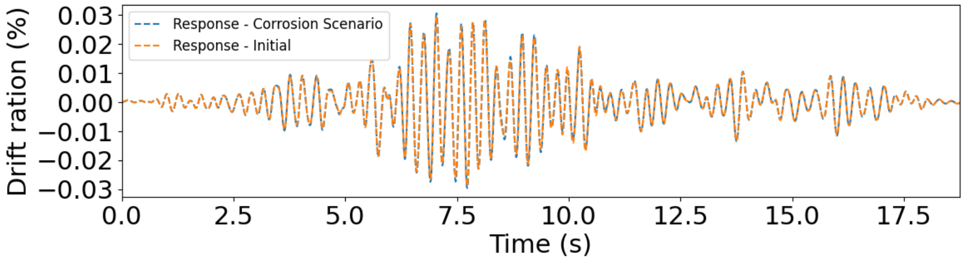

(a) Prediction to ground motion with the initial FEA model (PGA = $0.05g$).

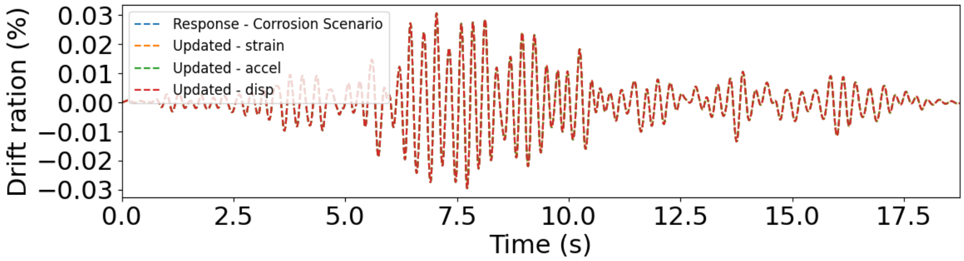

(b) Prediction to ground motion using the updated FEA model, in unforseen data (PGA = $0.05g$).

Figure 7: Comparison of the prediction of the initial and updated FEA model to unforseen ground motion (PGA = $0.05g$).

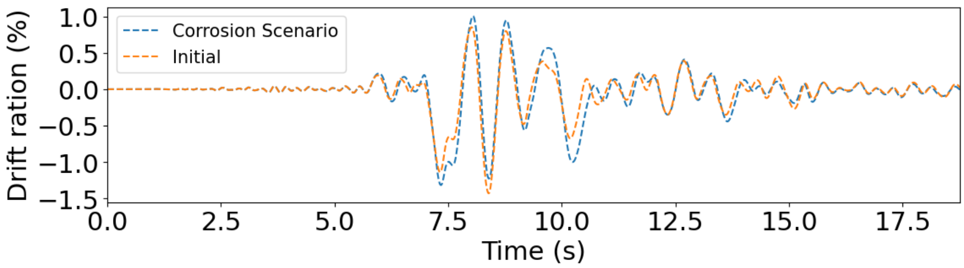

(a) Prediction to ground motion with the initial FEA model (PGA = $0.24g$).

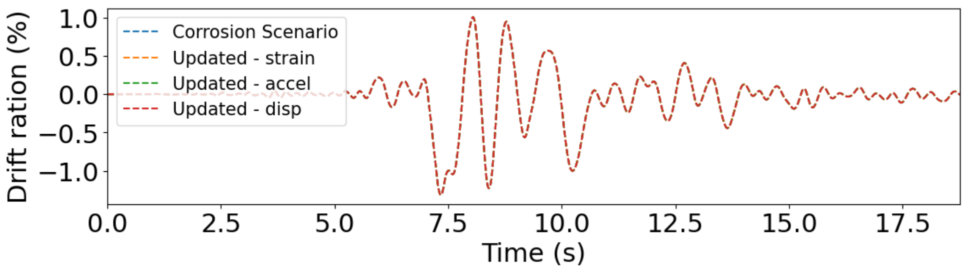

(b) Prediction to ground motion using the updated FEA model, in unforseen data (PGA = $0.24g$).

Figure 8: Comparison of the prediction of the initial and updated FEA model to unforseen ground motion (PGA = $0.24g$).

Figure 9 presents the fragility curves corresponding to a drift threshold of 0.020 (2%) for the case of PGA = 0.24g. The "Initial" curve, obtained prior to updating, shows a noticeably shifted response, underestimating failure probability at lower intensity levels and overestimating it at higher ones. After updating with different measurement types (strain, acceleration, and displacement), the fragility curves converge closely toward the "True" reference curve. This convergence demonstrates that model updating substantially improves the accuracy of fragility prediction, regardless of the measurement type employed, and reduces the bias present in the initial model.

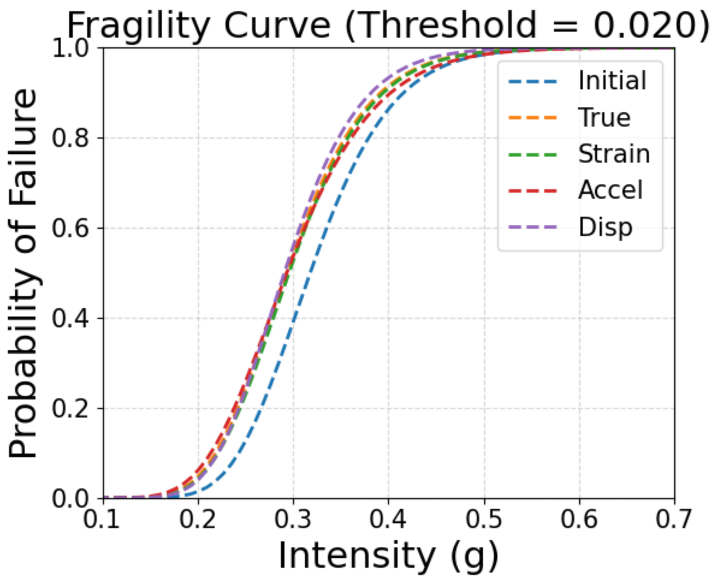

Figure 9: Initial and updated fragility curves at a drift-ratio threshold of 0.02 (2%) for different measurement types; case with PGA = 0.24g.

5 CONCLUSIONS

This work presented a FEMU framework for corrosion-affected RC bridge piers that combines an online nonlinear FE model with an Unscented Kalman Filter (UKF) and a probabilistic, time-dependent corrosion model. Using a representative pier, we generated synthetic "measured" responses under two seismic intensity levels (PGA = 0.05g and 0.24g) and quantifie parameter influenc via tornado diagrams built from $\pm 10\%$ perturbations. Identifiabilit , depended on excitation level—at 0.05g the response was largely linear and only the rebar diameter could be isolated with confidence whereas at 0.24g the nonlinear response enabled reliable identificatio of both rebar diameter and f_y.

Model updating improved predictive accuracy on unforeseen ground motions. For the low-intensity case, the updated model reproduced the target response with an RMS error of 0.05% (down from 8.5% for the initial model), and for the higher-intensity case, the RMS error dropped from 46% to 0.10%. Beyond response matching, the framework also enhanced fragility prediction. As shown in Figure 9, the initial fragility curve deviated significantl from the reference, particularly at intermediate intensity levels. After updating with different measurement types (strain, acceleration, displacement), the fragility curves aligned closely with the "True" curve, demonstrating that the proposed methodology not only calibrates structural parameters but also yields accurate probabilistic capacity estimates.

Overall, the results confir that (i) corrosion-related reinforcement parameters are both influentia and identifiable (ii) sufficien seismic demand is essential to activate nonlinear mechanisms needed for full parameter recovery, and (iii) the UKF-based FEMU framework substantially improves both deterministic response predictions and probabilistic fragility assessments. These finding highlight the potential of the method for structural health monitoring and seismic risk evaluation of aging RC bridge piers, with future work directed toward validation with fiel data and system-level applications.

6 ACKNOWLEDGMENT

The research project was supported by the Hellenic Foundation for Research and Innovation (H.F.R.I.) under the "2nd Call for H.F.R.I. Research Projects to support Faculty Members & Researchers" (Project Number: 04140).

REFERENCES

[1] E.A. Wan, R. Van Der Merwe, The unscented Kalman filte for nonlinear estimation. *Proc. IEEE Adaptive Systems for Signal Processing, Communications, and Control Symposium*, Lake Louise, Canada (2000), 153–158. https://doi.org/10.1109/ASSPCC.2000.882463

[2] M. Fragiadakis, I. Prentzas, M. Georgioudakis, S. Diamantopoulos, O. Markogiannaki, S. Stefanidou, Integration of measured data for the seismic fragility assessment of deteriorated bridges. *EuroStruct 2023 Eur. Assoc. Qual. Control Bridges Struct. Digit. Transf. Sustain.*, 6(5) (2023), 1377–1381. https://doi.org/10.1002/cepa.2207

[3] S. Abtahi, Z. Liu, Y. Li, Corrosion-related parameter estimation for RC structures using UKF-based Bayesian nonlinear finit element model updating with seismic data. *Mech. Syst. Signal Process.*, 191 (2023), 110169. https://doi.org/10.1016/j.ymssp.2023.110169

[4] C.-S. Shim, N.-S. Dang, S. Lon, C.-H. Jeon, Development of a bridge maintenance system for prestressed concrete bridges using 3D digital twin model. *Struct. Infrastruct. Eng.*, **15**(10), 1319–1332, 2019.

[5] S. Jang, J. Li, B.F. Spencer, Corrosion estimation of a historic truss bridge using model updating. *J. Bridge Eng.*, **18**(7), 678–689, 2013.

[6] S.A. Faroz, N.N. Pujari, S. Ghosh, Reliability of a corroded RC beam based on Bayesian updating of the corrosion model. *Eng. Struct.*, **126**, 457–468, 2016.

[7] M. Hoshiya, E. Saito, Structural identificatio by extended Kalman filte . *J. Eng. Mech.*, **110**, 1757–1770, 1984.

[8] E.N. Chatzi, A.W. Smyth, The unscented Kalman filte and particle filte methods for nonlinear structural system identificatio with non-collocated heterogeneous sensing. *Struct. Control Health Monit.*, **16**, 99–123, 2009.

[9] R. Astroza, H. Ebrahimian, J.P. Conte, Material parameter identificatio in distributed plasticity FE models of frame-type structures using nonlinear stochastic filtering *J. Eng. Mech.*, **141**, 4014149, 2015.

[10] I. Prentzas, M. Fragiadakis, Quantifie active learning Kriging model for structural reliability analysis. *Probab. Eng. Mech.*, 78 (2024), 103699. https://doi.org/10.1016/j.probengmech.2024.103699

[11] I. Prentzas, S. Diamantopoulos, M. Fragiadakis, Multi-hazard fragility updating using structural health monitoring. *Proc. 18th World Conf. Earthq. Eng. (WCEE2024)*, Milan, Italy, June 30–July 5, 2024. https://proceedings-wcee.org/view.html?id=23310 & conference=18WCEE

[12] DuraCrete, Statistical quantificatio of the variables in the limit state functions. The European Union Brite EuRam 3 contract BRPR-CT95-0132 Project BE95-1347 Report no BE95-1347/R7. (2000).

[13] M.G. Stewart, D.V. Rosowsky, Time-dependent reliability of deteriorating reinforced concrete bridge decks. *Struct. Saf.*, 20(1) (1998), 91–109.

[14] M. Fragiadakis, D. Vamvatsikos, Fast performance uncertainty estimation via pushover and approximate IDA. *Earthq. Engng. Struct. Dyn.*, 39 (2010), 683–703. https://doi.org/10.1002/eqe.965

[15] M. Zhu, F. McKenna, M.H. Scott, OpenSeesPy: Python library for the OpenSees finit element framework. *SoftwareX*, 7 (2018), 6–11. https://doi.org/10.1016/j.softx.2017.10.009